Arsenic redistribution at the SiO_2/Si interface during oxidation of implanted silicon

Fabio Iacona, Vito Raineri, and Francesco La Via
CNR-IMETEM, Stradale Primosole 50, 95121 Catania, Italy

Antonio Terrasi and Emanuele Rimini
INFM and Dipartimento di Fisica dell'Università, Corso Italia 57, 95129 Catania, Italy
(Received 13 April 1998)

The behavior of ion-implanted As in (100) silicon wafers, following thermal oxidation, has been investigated by Rutherford backscattering spectroscopy, atomic force microscopy, transmission electron microscopy, and extended x-ray-absorption fine structure. The adopted fluences (3×10^{15} and 3×10^{16} cm^{-2}) and oxidation conditions (wet 920 °C, dry 1100 °C) span quite a broad range of phenomena, giving rise to As diffusion in the bulk, and/or segregation and precipitation at the SiO_2/Si interface. The surface roughness is correlated to that measured at the interface, although the oxide presence strongly reduces the value with respect to that present at the interface. Rough interfaces and surfaces are formed when the arsenic concentration exceeds the solid solubility and precipitation occurs. The SiAs precipitates are characterized by a monoclinic structure with low surface energy for the (100) facet, as determined by the Wulff plot. Residual roughness is left at the oxide surface even if precipitates initially formed dissolve during subsequent oxidation. The depth profile of the dopant has been quantitatively computed by the analytical solution of the diffusion equation, taking into account the interface movement, the As redistribution at the interface between oxide and bulk silicon, the formation, growth, and dissolution of precipitates, and, of course, the drive-in process. The dependence of the diffusion coefficient on the dopant concentration has been also considered and determined as a converging parameter, considering iteratively the differential equation solution. In all the investigated cases the agreement between experimental data and calculations has been found to be good. [S0163-1829(98)08539-7]

I. INTRODUCTION

The behavior of the most common dopants during thermal oxidation of silicon has been extensively studied, due to its tight correlation with the doped silicon electrical properties.[1–3] Indeed, during the SiO_2/Si interface movement toward bulk silicon, impurities can be embedded in the SiO_2 layer or can pile up at the interface. These phenomena are quantitatively described by the segregation coefficient, defined as the equilibrium ratio between impurity concentration in the silicon and in the oxide.[1] Among the most common dopants, B has a segregation coefficient lower than 1, i.e., it is preferentially embedded in the oxide, while As, Sb, and P have a segregation coefficient higher than 1, i.e., they segregate at the interface during the oxidation process. From the electrical point of view, both situations cause a loss of dopant, because the atoms segregating at the interface form precipitates when their concentration exceeds the solid solubility.

More recently, the relationship between impurity segregation phenomena and morphology of the SiO_2 layers formed by thermal oxidation has been investigated in detail. The formation of precipitates at the SiO_2/Si interface has been observed for silicon implanted with Pb, Ag, and other metals,[4] As,[5,6] and Ge.[6,7] Moreover, the formation of SiO_2 layers having a rough surface has been related to the SiO_2/Si interface morphology.[6] In the case of Ge-implanted silicon, the formation of precipitates has been found to depend on the implanted dose. Oxidation of samples implanted with 3×10^{15} Ge/cm^2 does not lead to precipitate formation, while the phenomenon is clearly visible when samples implanted with higher doses (1×10^{16} and 3×10^{16} cm^{-2}) are oxidized. The low-dose behavior has been explained through the capability of the segregating Ge atoms to form flat and well-ordered Ge_xSi_{1-x} layers; when the concentration of segregating atoms becomes too high, ordered layers cannot anymore be formed, and precipitation occurs.[6]

In the case of As-implanted silicon, precipitation occurs already at 3×10^{15} cm^{-2}, due to the relatively low As solubility. The phenomenon has been found to be strongly temperature dependent;[5,6] indeed, low-temperature oxidation (920 °C) produces SiO_2 layers having a roughness higher than 0.5 nm (i.e., about five times higher than that detected on oxides grown under the same conditions on unimplanted silicon). On the other hand, by increasing the oxidation temperature up to 1100 °C, the surface roughness becomes comparable to that of oxides grown on virgin silicon. Arsenic behavior has been qualitatively explained in terms of the competition between As diffusion rate, prevailing at 1100 °C, and the silicon oxidation rate, prevailing at 920 °C.[6]

In this paper we discuss the As precipitation at the SiO_2/Si interface during thermal oxidation of As-implanted silicon. In particular, we have first investigated the influence of different oxidation conditions and implanted doses on the As redistribution during silicon thermal oxidation; the related formation of As-containing precipitates has been discussed on the basis of Rutherford backscattering spectrometry (RBS), atomic force microscopy (AFM), transmission electron microscopy (TEM), and extended x-ray-absorption fine-structure (EXAFS) measurements. The observed interface

0163-1829/98/58(16)/10990(10)/$15.00 PRB 58 © 1998 The American Physical Society

roughening has been related to the As homogeneous precipitation at the interface. Furthermore, we have identified the presence of the monoclinic SiAs phase in silicon, so far rarely observed, even if early described,[8] and obtained fundamental properties on SiAs precipitates, including the surface free-energy plot. Finally, a model that accurately describes the As behavior during the oxidation process is also presented. This model, based on the solution of the diffusion differential equation, with suitable boundary conditions, has been employed to obtain theoretical As profiles and interface concentrations that have been compared with the experimental data.

II. EXPERIMENTAL DETAILS

As ions were implanted at an energy of 70 keV into Czochralski-grown (100) or (111) silicon wafers to doses of 3×10^{15} and 3×10^{16} ions/cm^2, with a peak concentration of $\approx5\times10^{20}$ and 5×10^{21} atoms/cm^3, respectively. These concentrations are higher than the As solid solubility in silicon (2×10^{20} atoms/cm^3 at 920 °C and 4×10^{20} atoms/cm^3 at 1100 °C).[9]

Before oxidation the wafers were cleaned by a standard RCA procedure to reduce the surface contamination. The surface morphology has been checked before and after RCA cleaning, demonstrating its ineffectiveness in changing surface characteristics.

The wafers have been loaded in a horizontal furnace at 800 °C, then the temperature has been raised at a rate of 10 °C/min up to 920 or 1100 °C. During loading, temperature ramping up and unloading processing steps, wafers were held in N_2. The implantation process produced an amorphous surface layer 100 nm thick, that epitaxially regrows at 800 °C with rates of about 10^3 and 50 nm/s, for (100) and (111) orientations, respectively. This means that the complete recrystallization of the substrate has been obtained in a few seconds at the loading temperature (800 °C). This temperature still prevents competition between solid phase epitaxy (SPE) and local diffusive rearrangements, that can lead to polysilicon formation or As segregation phenomena.[10] The absence of segregation due to SPE has been also confirmed in samples annealed in N_2 at 920 or 1100 °C by As depth profiles carried out by RBS.

Oxidation has been performed, for times ranging between 1 and 120 min, at 920 °C in a wet environment (H_2O vapor formed by the pyrogenic technique), and at 1100 °C in dry oxygen. The two processes are characterized by the same oxidation rate for unimplanted silicon wafers, because the difference in temperature balances the effect of the oxidizing species concentration (at the same temperature H_2O concentration in the growing SiO_2 layer during wet oxidation is about three orders of magnitude higher than O_2 concentration during dry oxidation).[11] Further, the presence of As greatly enhances the wet oxidation rate (up to a factor of 7 with respect to that of unimplanted silicon), while the dry oxidation rate is only slightly affected.[12,13]

The SiO_2/Si structures have been characterized by AFM and TEM measurements, while the As profile and its surrounding was determined by 2.0-MeV He^+ ions by RBS and EXAFS measurements. The oxide thickness was measured by ellipsometry, and the results compared with TEM and RBS measurements.

A Digital Instrument Nanoscope III-AFM, in tapping mode configuration, was used to obtain 5×5 and 1×1-μm^2 images of the SiO_2 surfaces. The SiO_2/Si interfaces have been analyzed by AFM after removal of the oxide layers by dipping in a diluted (4%), buffered HF solution. The root-mean-square (rms) of the AFM height data, taken from 5×5-μm^2 scans, is reported in the following as the roughness value. For the analyzed area the rms data are size independent, the correlation length being lower than 2 μm in all the cases investigated. The roughness data accuracy, tested on different regions of the same sample and on several identically prepared samples, was better than 20%.

Cross-section TEM analyses were carried out in a Jeol 2010 FX microscope, operating at 200-kV accelerating voltage, in the pole configuration to avoid sample tilting effects on the precipitate shape.

EXAFS measurements were performed at the European Synchrotron Radiation Facility (ESRF) in Grenoble (France) using the Italian beam line GILDA. Quantitative EXAFS data analysis was obtained by back-transforming the peak of the first coordination shell and fitting the signal with phases and amplitudes obtained from reference samples.

III. RESULTS AND DISCUSSION

A. As redistribution and precipitation—experimental data

The arsenic redistribution caused by silicon thermal oxidation has been analyzed by the RBS technique. The spectrum of a sample implanted with 70-keV 3×10^{16} As/cm^2, and after wet oxidation at 920 °C for 10 min is reported in Fig. 1(a). The Si and O signals indicate the presence of a SiO_2 layer 370 nm thick, while the sharp As peak located at the SiO_2/Si interface indicates the occurrence of As segregation. Only a very low As concentration is found in the oxide layer.

Figure 1(b) demonstrates the leading role played by temperature in determining the As profile. The RBS spectrum refers to an identical silicon sample but oxidized for 30 min at 1100 °C in a dry environment (an oxide thickness of 130 nm). The ineffectiveness of the chemical environment in determining As behavior during thermal oxidation has been already demonstrated.[5,6] The spectrum indicates the absence of As segregation; the atoms are indeed uniformly distributed inside the silicon substrate for at least a few hundred nanometers, as a result of the prevalence of diffusion over the oxidation rate. Also in this case, no appreciable As concentration has been detected in the oxide layer.

Table I summarizes the RBS results for different oxidation conditions and implanted doses. All the RBS aligned spectra have been collected after etching the SiO_2 layer in a diluted (4%) HF solution. The data indicate a low As concentration in all oxide layers, according to the As segregation coefficient.[1]

Under low-temperature oxidation, As atoms segregate at the SiO_2/Si interface; for the high-dose implant, the small difference between random and channeling RBS yields indicates that the segregated As atoms are mainly located in nonsubstitutional lattice sites. On the other hand, in low-dose implant samples, the As distributions are generally quite

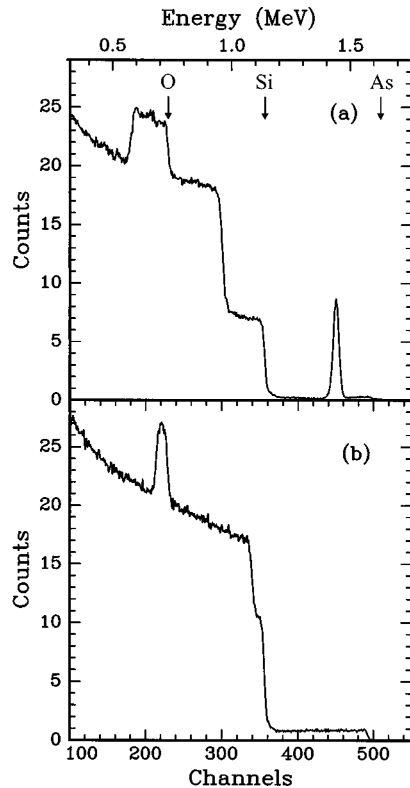

FIG. 1. RBS spectra of Si implanted with 70-keV 3×10^{16} As/cm^2, after (a) wet oxidation at 920 °C for 10 min, and (b) dry oxidation at 1100 °C for 30 min. The arrows indicate the surface markers of all elements.

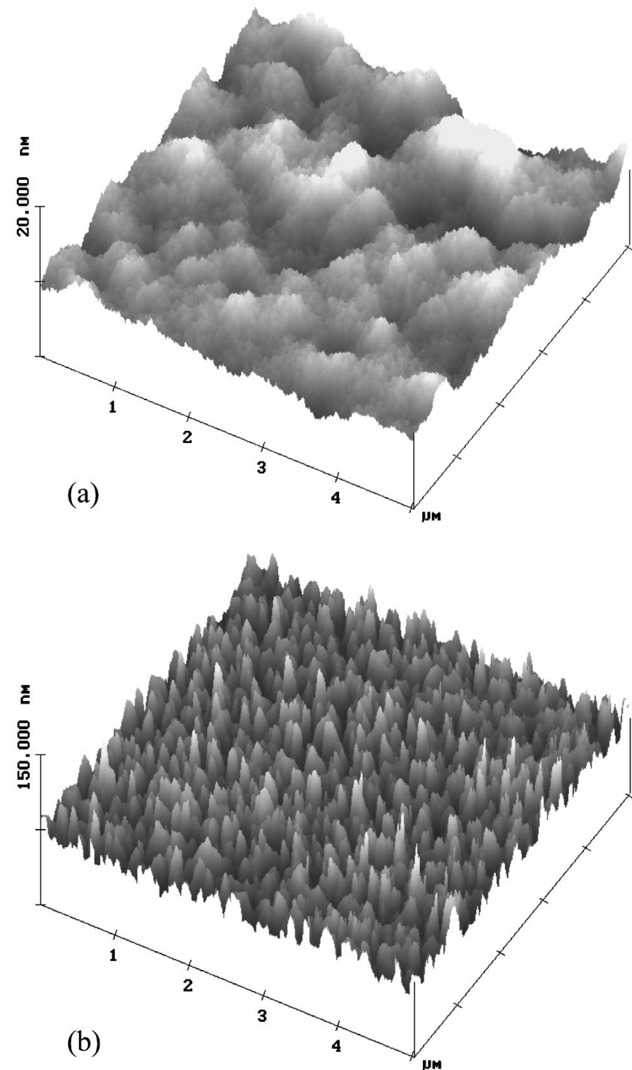

FIG. 2. AFM images of (a) the surface of a 370-nm-thick SiO_2 layer grown at 920 °C for 10 min on silicon implanted with 70-keV 3×10^{16} As/cm^2, and (b) the SiO_2/Si interface of the same sample, after etching the SiO_2 layer in HF.

broad, with a pronounced low-energy tail; under ion-channeling conditions, the intensities of these signals peaks are heavily attenuated, suggesting that a significant fraction of the As is located in substitutional lattice sites.

For the samples oxidized at high temperature, a quantitative analysis of the As signals is not possible, due to the overlap with the Si signal [see Fig. 1(b)]; however, within the uncertainties related to the As fraction not detectable by RBS measurement, the aligned contributions are quite low, suggesting that a large fraction of As atoms occupies substitutional lattice sites, as a result of diffusion processes.

The temperature of the oxidation process influences also the morphology of the SiO_2 layers grown on As-implanted silicon. The surface of a SiO_2 layer grown at 920 °C for 10 min on silicon implanted with 3×10^{16} As/cm^2 is characterized by a marked roughness [see the AFM image of Fig. 2(a)]. This surface morphology is due to the large SiO_2/Si interface roughness shown in the AFM image of Fig. 2(b), obtained after HF etching of the oxide; note that the z axis scale of Fig. 2(b) has been increased by a factor of 7.5 with respect to that of Fig. 2(a). Furthermore, the TEM cross sec-

TABLE I. As surface concentrations in Si and SiO_2, determined by RBS measurements performed in random and aligned configurations, for different implanted doses and oxidation conditions.

	Oxidation parameters			C_{As}(cm^{-2})		
As dose	Temp.	Time	Thickness	Si		SiO_2
(cm^{-2})	(°C)	(min)	(nm)	Random	Aligned	Random
3×10^{15}	920	10	180	3.1×10^{15}	1.3×10^{15}	n.d.
3×10^{15}	920	30	270	3.4×10^{15}	1.4×10^{15}	n.d.
3×10^{16}	920	10	370	2.8×10^{16}	2.7×10^{16}	4.9×10^{15}
3×10^{16}	920	30	550	3.0×10^{16}	2.9×10^{16}	1.6×10^{15}
3×10^{15}	1100	30	100	$\sim2.0\times10^{15}$	$\sim6.0\times10^{14}$	n.d.
3×10^{16}	1100	30	130	$\sim2.0\times10^{16}$	$\sim2.0\times10^{15}$	n.d.

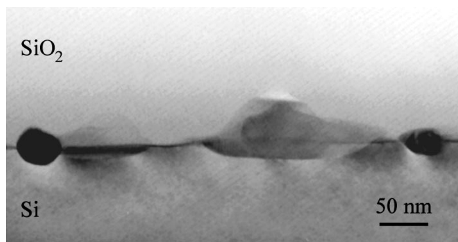

FIG. 3. TEM cross section of the interface between a 370-nm-thick SiO_2 layer grown at 920 °C for 10 min on silicon implanted with 70-keV 3×10^{16} As/cm^2 and the silicon substrate.

tion of Fig. 3 demonstrates the presence of a large number of precipitates at the SiO_2/Si interface. Because RBS analyses, performed before and after SiO_2 etching, demonstrate that this procedure does not change appreciably the As content of the sample, we can associate the morphology shown in Fig. 2(b) with the precipitates shown in Fig. 3. Therefore, on the basis of the AFM, TEM, and RBS data, one can conclude that As segregation leads to an interface As concentration higher than its solid solubility, and then to precipitate formation at the SiO_2/Si interface. Notwithstanding their distance from the oxide surface, these precipitates greatly influence the morphology of the SiO_2 layer. However, the interface roughness is not perfectly reproduced, in both morphology and absolute value, on the oxide surface, because the planarization properties of the oxide smooth the interface asperity.

Figure 4(a) shows that the roughness detected by AFM on

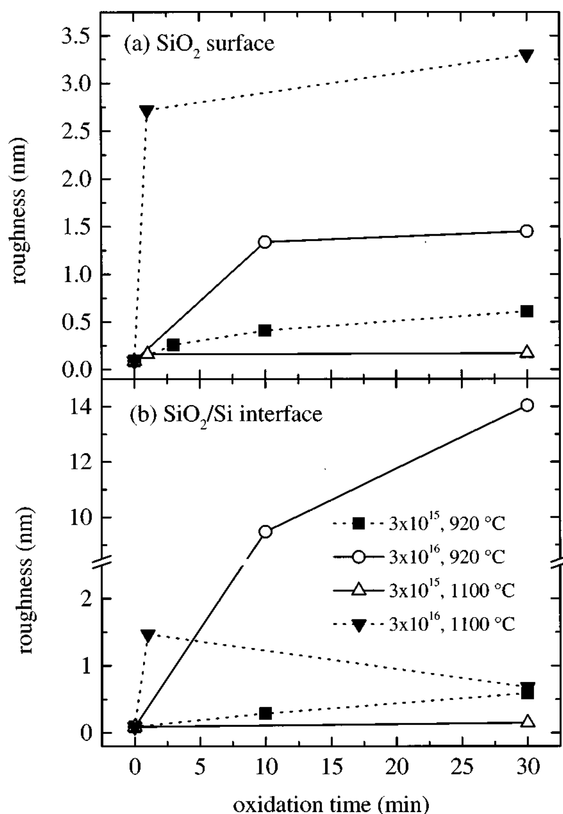

FIG. 4. Roughness (rms) as a function of the oxidation time for (a) the surface of oxides grown on As-implanted silicon, and (b) the SiO_2/Si interface after SiO_2 etching.

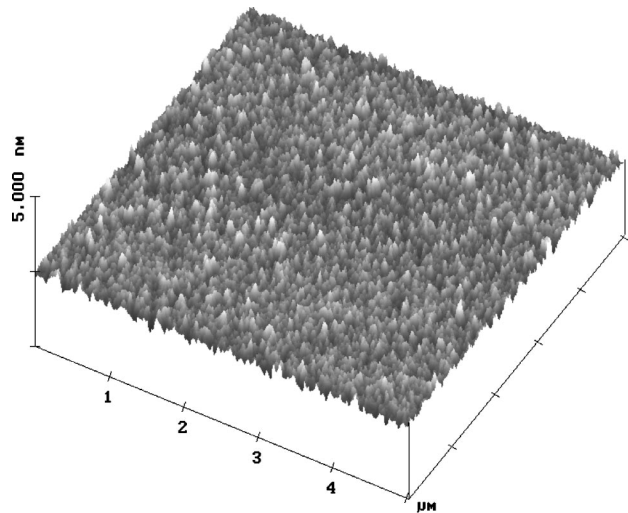

FIG. 5. AFM surface image of a 100-nm-thick SiO_2 layer grown at 1100 °C for 30 min on silicon implanted with 70-keV 3×10^{15} As/cm^2.

the surface of the oxides grown at 920 °C increases with the implanted dose and, for the same dose, with the oxidation time, because both situations involve the accumulation at the interface of larger amounts of As atoms. For comparison, the surface roughness of oxides grown under the same conditions on unimplanted silicon is about 0.1 nm.[5,6] Larger roughness values and a more marked dependence are shown in Fig. 4(b), referring to the interface. This is due to the fact that AFM is now able to detect the bared precipitates, without the above-mentioned planarization effect of the oxide.

RBS analysis has demonstrated that, during 1100 °C oxidation, As does not segregate at the interface. Accordingly, the AFM and TEM analyses reported in Figs. 5 and 6, respectively, show that a sample implanted with 3×10^{15} As/cm^2 and oxidized for 30 min does not show precipitates formation, but it is characterized by flat surface and interface. Figures 4(a) and 4(b) show that all the SiO_2 surfaces and SiO_2/Si interfaces obtained by 1100 °C oxidation of samples implanted with 3×10^{15} As/cm^2 are very flat, independent of the oxidation time.

On the other hand, Figs. 4(a) and 4(b) indicate that 1100 °C oxidation of 3×10^{16} As/cm^2 implanted samples leads unexpectedly to the formation of rough surfaces and interfaces, even if no As accumulation at the interface is measured by the RBS spectrum of Fig. 1(b), clearly indicating the occurrence of As diffusion. Figure 7(a) reports the AFM image of the surface of an oxide layer grown at 1100 °C for 30 min, demonstrating that the high roughness

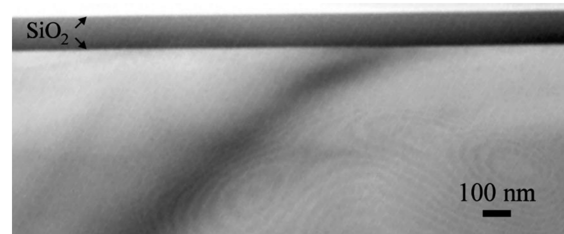

FIG. 6. TEM cross section of a SiO_2 layer grown at 1100 °C for 30 min on silicon implanted with 70-keV 3×10^{15} As/cm^2.

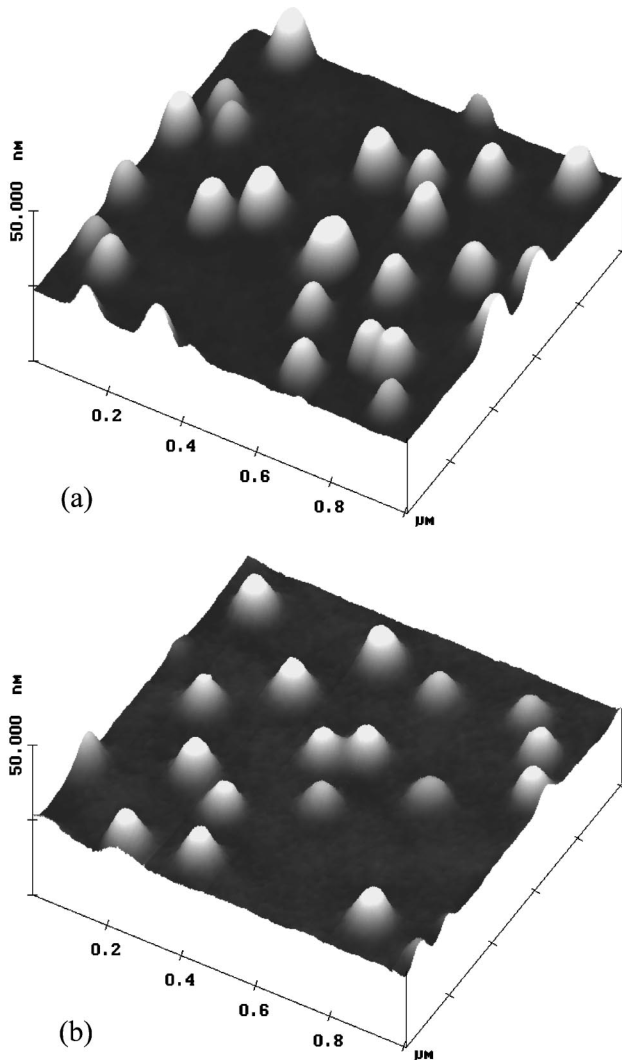

FIG. 7. AFM surface images of SiO_2 layers grown at 1100 °C (a) for 30 min (thickness of 130 nm), and (b) for 1 min (thickness of 25 nm), on silicon implanted with 70-keV 3×10^{16} As/cm^2.

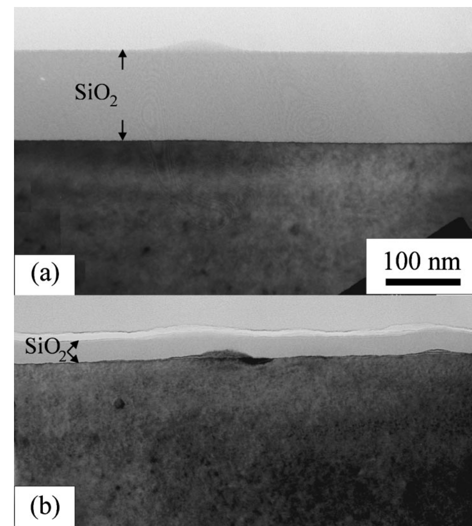

FIG. 8. TEM cross sections of SiO_2 layers grown at 1100 °C (a) for 30 min and (b) for 1 min on silicon implanted with 70-keV 3×10^{16} As/cm^2.

value is due to a peculiar SiO_2 morphology, that, on the analogy of 920 °C oxidations, could suggest the presence of precipitates. On the other hand, contrary to the case of 920 °C oxidations, the relative TEM cross section, reported in Fig. 8(a), shows that the interface with the Si substrate is very flat; this cross section evidences also the presence of the same surface features already detected by AFM analysis. The AFM image of the interface (not shown) confirms the TEM data.

The analysis of the sample in the early stages of the oxidation process enlightens the situation. The AFM image reported in Fig. 7(b), taken just after oxidation at 1100 °C for 1 min, shows that the peculiar SiO_2 morphology is already developed; on the other hand, the TEM cross section of Fig. 8(b) shows that in this case there exists a clear correspondence between the surface and interface morphologies.

Therefore, the analysis of all data suggest that, at this high dose, the As concentration at the interface in the early stages of the oxidation process performed at 1100 °C can exceed the solid solubility before significant diffusion occurs; consequently, precipitates are formed, and interface and surface morphology are affected [see the very high roughness of these samples in Figs. 4(a) and 4(b)]. Note that the oxide of Fig. 7(b) is only 25 nm thick; this explains the absence of any planarization effect. As oxidation is performed for longer times, the high As diffusivity leads to precipitate dissolution, and then to the recovery of a flat interface; however, the plastic deformation of the oxide during the precipitate formation in the early stages of the oxidation cannot be completely recovered, and oxides retain the old morphology.

B. Precipitate structure and facet shape

The structure of the As-containing precipitates has been investigated by EXAFS analysis performed at the As *K*-edge (11 881 eV). By a suitable analysis of the data, the local coordination (atomic species, coordination number, and nearest-neighbor distances) around the probed sites can be determined.[14] In particular, the Fourier transform (FT) of the EXAFS signal generates a number of peaks reproducing the radial distribution function around the investigated atoms. In our case, peaks will be centered at the interatomic distances between As and neighboring atoms, shortened by a small amount known as the phase shift. As an example, the FT of two different samples are reported in Fig. 9: (a) a sample implanted with 3×10^{15} As/cm^2 and annealed in N_2 at 1100 °C for 100 s (continuous line); and (b) a sample implanted with 3×10^{16} As/cm^2 and oxidized at 920 °C for 10 min (dashed line). The first sample was used as reference for As in a substitutional-like configuration. The crystalline quality of this sample was checked by TEM and RBS (not shown here); no precipitates and a $\chi_{\rm min}$ as low as 3% in channelling RBS were found. Moreover, four-point probe electrical measurements (not reported) confirm that all the As is electrically active, as well established for this dose and thermal process.[15] This scenario is in agreement with the FT, showing three atomic shells around As, indicating a very high structural order in this sample. Consequently, the peaks in the FT correspond to four Si first neighbors at 2.41 Å, 12 Si second neighbors at 3.84 Å, and 12 Si third neighbors at 4.50 Å (i.e., As in substitutional sites).[16] The other FT of Fig. 9 (dashed line) has a single peak, indicating a quite disor-

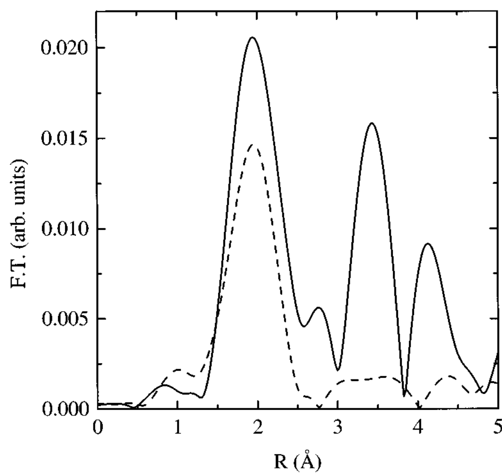

FIG. 9. Fourier-transform amplitudes of the EXAFS signals of a sample implanted with 3×10^{15} As/cm^2 and annealed in N_2 at 1100 °C for 100 s (continuous line), and a sample implanted with 3×10^{16} As/cm^2 and oxidized at 920 °C for 10 min (dashed line).

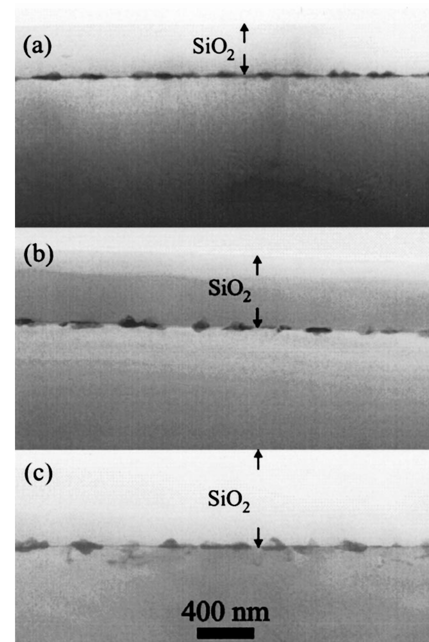

FIG. 10. TEM cross sections of silicon implanted with 70-keV 3×10^{16} As/cm^2 after wet oxidation at 920 °C (a) for 10 min, (b) for 30 min, and (c) for 120 min.

dered configuration around As atoms. This sample, in fact, exhibits the typical configuration of the monoclinic SiAs structure, with three Si atoms at an average distance of 2.38 Å, which is the result of three different As sites, each one having $2+1$ or $1+2$ Si first neighbors at slightly different distances.[16,17] The second coordination shell of the monoclinic SiAs structure is also made by several sites occupied by both As and Si atoms. This high static disorder explains the presence of a single peak in the FT signal. Using the first sample of Fig. 9 as a reference for the As-Si coordination, and EXAFS data (not shown) on As powder as reference for eventual As-As coordination, we have fitted all experimental data. Results can be summarized as follows.

(a) All the oxidized samples are better fitted when the presence of about 10% of As in first coordination is included. These As-As bonds can be associated to the presence of pure As or $SiAs_2$ precipitates.[18]

(b) Samples processed at 1100 °C have 90% of As coordinated with four Si atoms in a substitutional-like configuration regardless of the implantation dose. This confirms that the morphology of the sample implanted with 3×10^{16} cm^{-2} and oxidized for 30 min, reported in Fig. 7(a), is not due to the presence of precipitates, revealing a very ordered structure, with As in substitutional-like configuration.

(c) Samples processed at 920 °C show 90% of monoclinic SiAs precipitates in the case of high implantation dose, while As in substitutional sites, and SiAs precipitates, coexist in low dose samples.

A detailed description of the EXAFS data is published elsewhere.[19]

As discussed above, arsenic accumulation at the interface takes place during oxidation at 920 °C the As diffusivity being smaller than the interface velocity. Longer oxidation times increase the amount of As accumulated at the interface, and precipitation occurs when the solid solubility is exceeded. Homogeneous precipitation induces formation of single precipitates that, at equilibrium, have a well-defined shape, determined by their surface energy, according to the Wulff construction. At equilibrium all the precipitates have the same shape, independently of their sizes.[20]

Figures 10(a), 10(b), and 10(c) show the TEM cross sections of the 3×10^{16}-cm^{-2} As-implanted sample after oxidation processes performed at 920 °C for 10, 30, and 120 min, respectively. The micrographs show that the agglomeration process leads to the formation of large and isolated grains. Their shape indicates that the equilibrium conditions are reached just after short oxidation times. The same shape for the precipitates has been found also when (111) wafers were oxidized. Even if the (111) plane is parallel to the interface, a layer-by-layer precipitation does not occur. Isolated agglomerates are formed to minimize the surface energy of the nucleated precipitates. Then, the Wulff construction can be used to extract the complete surface free-energy plot of the SiAs precipitates.

SiAs precipitates present a monoclinic crystal structure, and they are coherent to the silicon crystal.[21] They lie in the {111} planes of silicon, and have a (001) plane parallel to the (111) plane of silicon.

The structure of a single precipitate can be better resolved in high TEM magnification reported in Fig. 11, referring to a sample implanted with 3×10^{16} As/cm^2 and oxidized at 920 °C for 120 min. In the image, well-defined {100} facets and other smaller curved facets are visible. Although the precipitates are in part embedded in the oxide layer and in part in the silicon, no clear differences have been observed in precipitate faceting between the two surfaces.

From the shape of the precipitates we can extract quantitative data on the surface free energy $\gamma(\vartheta)$ by using the Wulff construction.[22] In fact, we considered the SiAs/SiO_2 and the SiAs/Si facets separately. The Wulff point of a precipitate is defined as the intersection of the perpendicular bisectors of two {100} SiAs facets with the same material (oxide or silicon). Since there are no sharp facet intersec-

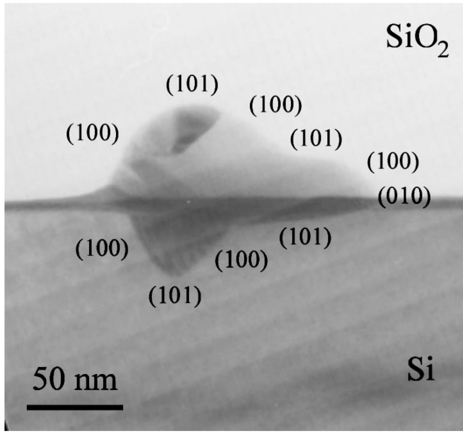

FIG. 11. Cross-section TEM analysis showing a SiAs precipitate at the SiO_2/Si interface. The oxide layer has been grown at 920 °C for 120 min on silicon implanted with 70-keV 3×10^{16} As/cm^2.

tions, $\gamma_i/r_i=$const, and we can measure the precipitate radius r_i to each of the surface orientations i and, consequently, extract the relative γ_i for each orientation. The precipitate radii are measured with steps of 2°.

The surface energy plot $\gamma(\vartheta)$, averaged and symmetrized on several precipitates, is shown in Fig. 12 for the SiAs/SiO_2 interface. Indeed, no difference was found on the surface energy plot for the two interfaces. According to the qualitative features deduced by the precipitate shape, a clear cusp has been detected only for the {100} planes, while no minimum was detected for the {010} and the {101} planes.

The surface energy ratio between the {101} and the {100} planes is high ($\gamma_{\{101\}}/\gamma_{\{100\}}=1.25$), so that the elongation along the {100} planes is quite advantageous. The plane {101} is rounded because its energy is small, while no evidence of other minima along intermediate orientations is present. The surface energy for the {010} plane is high with respect to the {100} ($\gamma_{\{010\}}/\gamma_{\{100\}}=1.28$).

C. As redistribution and segregation—model and comparison with experimental data

In the previous sections the morphology of SiO_2 layers and SiO_2/Si interfaces after oxidation of As-implanted silicon samples has been related to the dopant redistribution occurring during the process. The As concentration profile results from the competition between the silicon oxidation rate (prevailing at low temperature) and the As diffusion (prevailing at high temperature). In this section we will develop a model that quantitatively describes this process, providing a physical explanation to all our experimental results, including those in apparent contrast with the above exposed simple reasoning (i.e., As precipitation during 1100 °C oxidation of samples implanted with 3×10^{16} cm^{-2}).

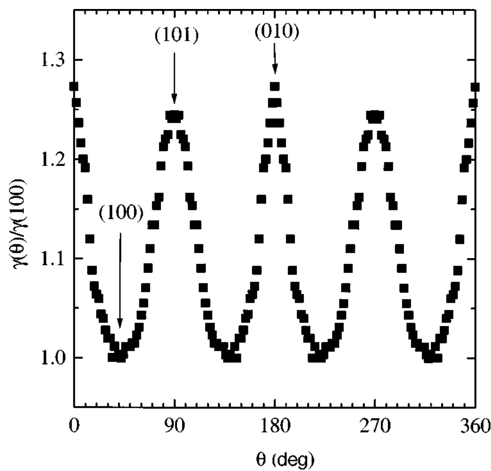

FIG. 12. The energy surface plot $\gamma(\vartheta)$ for the SiAs precipitates, obtained from the Wulff construction.

The As concentration in silicon, $C_{\mathrm{Si}}^{\mathrm{As}}(x,t)$, is provided by the solution of the diffusion differential equation

$$\frac{\partial C_{\mathrm{Si}}^{\mathrm{As}}(x,t)}{\partial t}=D_{\mathrm{Si}}^{\mathrm{As}}\frac{\partial^2 C_{\mathrm{Si}}^{\mathrm{As}}(x,t)}{\partial x^2} \quad (1)$$

($D_{\mathrm{Si}}^{\mathrm{As}}$ is the As diffusion coefficient in Si) with the following boundary conditions:

(i) The dopant segregation at the SiO_2/Si interface requires.

$$C_{\mathrm{Si}}^{\mathrm{As}}(0,t)=K_S C_{\mathrm{SiO_2}}^{\mathrm{As}}(0,t), \quad (2)$$

K_S being the segregation coefficient, and $C_{\mathrm{SiO_2}}^{\mathrm{As}}(x,t)$ the As concentration in SiO_2. The K_S value was assumed to be 50 for both temperatures.[1]

(ii) Mass conservation implies a flux equality at the interface:

$$D_{\mathrm{ox}}^{\mathrm{As}}\left(\frac{\partial C_{\mathrm{ox}}^{\mathrm{As}}}{\partial x}\right)_{x=0}=D_{\mathrm{Si}}^{\mathrm{As}}\left(\frac{\partial C_{\mathrm{Si}}^{\mathrm{As}}}{\partial x}\right)_{x=0}, \quad (3)$$

$$N_{\mathrm{Tot}}(t=0)=N_{\mathrm{Tot}}(t=t), \quad (4)$$

$D_{\mathrm{ox}}^{\mathrm{As}}$ being the As diffusion coefficient in SiO_2, and N_{Tot} the total As concentration in Si and SiO_2.

(iii) As precipitation occurs when the concentration exceeds the solid solubility value C_{SS} i.e.,

$$D_{\mathrm{Si}}^{\mathrm{As}}=0 \quad \text{if } C_{\mathrm{Si}}^{\mathrm{As}}>C_{SS}. \quad (5)$$

Moreover, the initial As distribution is described by a Gaussian, R_P and ΔR_p being the energy-dependent range and straggle of the implanted dopant ions:

$$C_{\mathrm{Si}}^{\mathrm{As}}(x,0)=\frac{N_{\mathrm{tot}}}{(2\pi)^{1/2}\Delta R_p}\exp\left[\frac{-(x-R_P)^2}{2\Delta R_p^2}\right]. \quad (6)$$

Since the diffusion equation and its associated boundary conditions are linear, the resulting impurity distribution is obtained by a linear combination of their solutions,[23] so that

$$C_{\mathrm{Si}}^{\mathrm{As}}(x,t)=C^1(x,t)+C^2(x,t)+C^3(x,t). \quad (7)$$

The function $C^1(x,t)$ is the solution of the diffusion equation and describes the thermal activated As diffusion inside silicon during oxidation ($C_{\max}$ is the peak value in the Gaussian distribution):[24]

$$C^1(x,t)=\frac{C_{\max}}{2(\pi D_{\mathrm{Si}}^{\mathrm{As}}t)^{1/2}}[\Omega(x+mx_0,t)+\beta_1\Omega(-x+mx_0,t)] \quad (8)$$

where

$$\beta_1=\frac{(D_{\mathrm{Si}}^{\mathrm{As}})^{1/2}-K_s(D_{\mathrm{ox}}^{\mathrm{As}})^{1/2}}{(D_{\mathrm{Si}}^{\mathrm{As}})^{1/2}+K_s(D_{\mathrm{ox}}^{\mathrm{As}})^{1/2}}, \quad (9)$$

$$\Omega(x,t)=C^{1/2}\exp\left[-\left(A-\frac{B^2}{4C}\right)\right]\frac{\pi^{1/2}}{2}\times\left(1+\mathrm{erf}\left\{\frac{x+mx_0-B/2}{C^{1/2}}\right\}\right), \quad (10)$$

$$A=\frac{(x+mx_0-R_P)^2}{2\Delta R_P}, \quad (11)$$

$$B=\frac{4D_{\mathrm{Si}}^{\mathrm{As}}t(x+mx_0-R_P)}{\Delta R_P^2+2D_{\mathrm{Si}}^{\mathrm{As}}t}, \quad (12)$$

$$C=\frac{4D_{\mathrm{Si}}^{\mathrm{As}}t\Delta R_P^2}{\Delta R_P^2+2D_{\mathrm{Si}}^{\mathrm{As}}t}, \quad (13)$$

$$x_0=\frac{k_P}{2k_1}\left\{\left[\frac{4(t+t^*)k_1^2}{k_P}\right]^{1/2}-1\right\}. \quad (14)$$

In the previous equations the coordinate x is measured from the position of the SiO_2/Si interface which changes during oxidation, and the term mx_0 accounts for the movement of the coordinate due to consumption of the substrate material. k_P and k_1 are, respectively, the experimental parabolic and linear oxidation rate constants, and t^* is the parameter related to the oxide thickness prior to oxidation. We assumed $t^*=0$ and $m=0.44$ for the ratio of consumed silicon thickness to the thickness of grown oxide.

The function $C^2(x,t)$ takes into account the mass conservation and describes the As redistribution due to the movement of the SiO_2/Si interface,[24]

$$C^2(x,t)=-\frac{K_S-m}{2}\left(\frac{\pi k_P}{D_{\mathrm{Si}}^{\mathrm{As}}\left(1+\frac{k_P}{4k_c^2t}\right)}\right)^{1/2}\times C_s\exp\left(\frac{mx_0}{2\sqrt{D_{\mathrm{Si}}^{\mathrm{As}}t}}\right)^2\mathrm{erfc}\left(\frac{x+mx_0}{2\sqrt{D_{\mathrm{Si}}^{\mathrm{As}}t}}\right), \quad (15)$$

the surface concentration C_S being given by

$$C_s=\frac{\frac{C_{\max}}{4\sqrt{D_{\mathrm{Si}}^{\mathrm{As}}t}}\Omega(mx_0,t)}{1+\frac{K_S-m}{2}\left(\frac{\pi k_P}{D_{\mathrm{Si}}^{\mathrm{As}}(1+k_P/4k_1^2t)}\right)^{1/2}\exp\left(\frac{mx_0}{2\sqrt{D_{\mathrm{Si}}^{\mathrm{As}}t}}\right)^2\mathrm{erfc}\left(\frac{mx_0}{2\sqrt{D_{\mathrm{Si}}^{\mathrm{As}}t}}\right)}. \quad (16)$$

The last term of Eq. (7), $C^3(x,t)$, describes the As behavior due to precipitates. Arsenic is immobile in a Gaussian distribution peaked at the average depth of the precipitate centers ($\bar{x}$) when its concentration exceeds the solid solubility. Moreover, arsenic diffuses from precipitates at the solid solubility values,[25]

$$C^3(x,t)=\frac{N_{\mathrm{prep}}}{\sqrt{2\pi D_{\mathrm{Si}}^{\mathrm{As}}t}}\exp\left\{-\frac{(x-\bar{x})^2}{2D_{\mathrm{Si}}^{\mathrm{As}}t}\right\}+C_{ss}[1-0.87E-0.45E^2], \quad (17)$$

N_{prep} being the amount of arsenic in the precipitates in at/cm^2,
and

$$E=2.3\left(\frac{C_{ss}D_{\mathrm{Si}}^{\mathrm{As}}t}{n_i}\right)^{1/2}\left(\frac{8C_{ss}}{n_i}D_{\mathrm{Si}}^{\mathrm{As}}t\right)^{-1/2}, \quad (18)$$

with n_i the intrinsic electron concentration at the diffusion temperature. $C^3(x,t)$ was neglected for As initial concentration below the solid solubility.

In the calculation, the dependence of the diffusion coefficient $D_{\mathrm{Si}}^{\mathrm{As}}$ on the As concentration was taken into account considering a vacancy-assisted mechanism,

$$D_{\mathrm{Si}}^{\mathrm{As}}=Dx+Dm\,\frac{C^1(x,t)}{n_i} \quad (19)$$

Dx and Dm being the contributions of the neutral and negative charged vacancies, respectively. The following values were adopted: $Dx=0.0116\exp(-3.44/(kT))$ and $Dm=31.62\exp[-4.15/(kT)]$.

Finally, arsenic concentration profiles were obtained by a self-consistent code developed to calculate the illustrated formula. The concentration values have been calculated starting from an initial profile to determine the diffusion coefficient, and then changing the diffusion coefficient using a converging criterion, so that the final distribution is determined when the difference between the initial and final profile becomes lower than 1%.

The comparison between the experimental As profile, obtained by RBS analysis, and the calculated $C_{\mathrm{Si}}^{\mathrm{As}}(x,t)$ concentration, is shown in Fig. 13 for samples implanted with 3×10^{16} As/cm^2, and oxidized for 30 min at 920 °C [Fig. 13(a)] and 1100 °C [Fig. 13(b)]. From the figures the very good agreement between calculated and experimental profiles is evident, demonstrating the capability of our model to describe the As depth distribution.

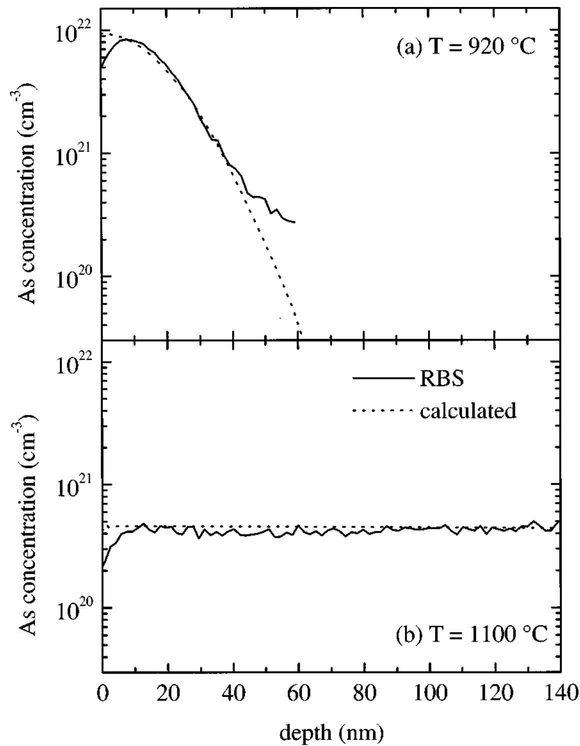

FIG. 13. RBS depth profiles and calculated As depth distribution of samples implanted with 70-keV 3×10^{16} As/cm^2 and oxidized for 30 min at (a) 920 °C and (b) 1100 °C.

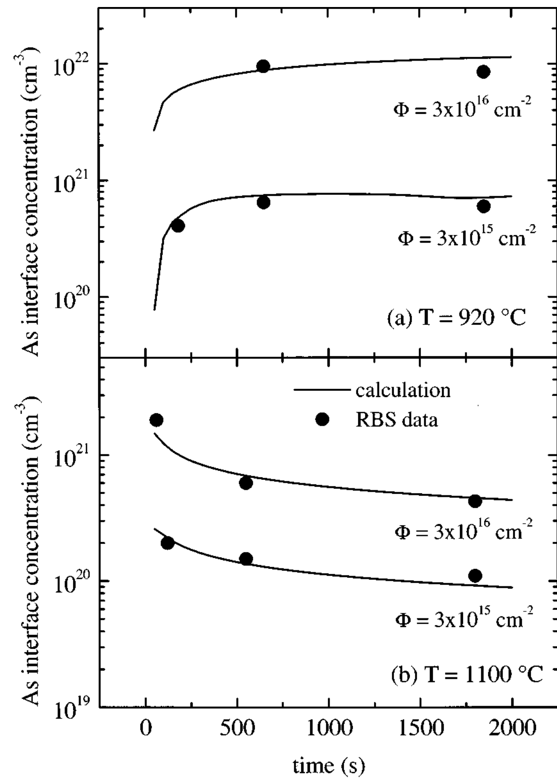

FIG. 14. Calculated interface As concentration (continuous line) and experimental values extracted from RBS data (dots) as a function of the oxidation time for (a) wet oxidation at 920 °C and (b) dry oxidation at 1100 °C of silicon implanted with 70-keV 3×10^{15} and 3×10^{16} As/cm^2.

The interface concentration values obtained from the calculated profiles have been used to build four curves, accounting for the variation of the As interface concentration as a function of the oxidation time for each temperature and implanted dose. In Figs. 14(a) and 14(b) we show the comparison between the calculated curves and the experimental values (extracted from RBS data) for all the investigated doses and temperatures. Also in this case the agreement is quite good.

Figure 14(a) shows that at 920 °C the As interface concentration rapidly increases in the first stages of the oxidation for both doses. After 300 s the interface concentration reaches a steady-state value of 7×10^{20} As/cm^3 (for the low dose) and 1×10^{22} As/cm^3 (for the high dose). Both experimental and calculated data show that these steady-state concentrations do not change for oxidation times as long as 2000 s. Because As solubility in silicon at 920 °C has a value of about 2×10^{20} atoms/cm^3, it can be concluded that, at 920 °C and for an implanted dose of 3×10^{15} cm^{-2}, As precipitation occurs for oxidation times higher than 60 s. On the other hand, for the implanted dose of 3×10^{16} As/cm^2, the interface As concentration immediately becomes higher than the As solid solubility, leading to precipitate formation.

At 1100 °C the As diffusivity is higher than the interface velocity. The As diffusion dominates the phenomenon and, for both doses, a decrease of the interface As concentration as a function of the oxidation time is observed [see Fig. 14(b)]. Because As solubility in silicon at 1100 °C has a value of about 4×10^{20} atoms/cm^3, it can be concluded that at 1100 °C and for a dose of 3×10^{15} cm^{-2} precipitation does not occur for all oxidation times, all values being lower than the solid solubility. On the other hand, for a dose of 3×10^{16} As/cm^2, the interface As concentration is higher than the As solid solubility in the early stages of the oxidation, leading to precipitate formation [see Fig. 8(b)]. At higher oxidation times, As atoms leave the interface region; this implies the dissolution of the SiAs precipitates [see Fig. 7(b)], in order to maintain in the silicon crystal an As concentration equal to its solid solubility.

IV. SUMMARY AND CONCLUSION

In this paper, As diffusion, segregation, and precipitation during oxidation was characterized and modeled. Arsenic accumulation at the SiO_2/Si interface has been determined by RBS measurements, while the precipitate formation has been monitored by AFM and cross section TEM analyses.

The As accumulated at the interface has a well-defined structure, as we could determine by morphological and structural investigations, mainly consisting of SiAs precipitates having a monoclinic crystal structure coherent with the silicon crystal.

Precipitate formation occurs due to homogeneous precipitation. From the precipitate shape we could determine the surface energy plot $\gamma(\vartheta)$ by Wulff construction. The surface energy ratio between the {101} and the {100} planes is high ($\gamma_{\{101\}}/\gamma_{\{100\}}=1.25$), so that elongation along the {100} planes is quite advantaged. The plane {101} is rounded because its energy is small, and no evidence of other minima along intermediate orientations has been observed. The surface energy consideration account for all the observed pre-

cipitate shapes and theoretically explain the interface roughening.

Homogeneous precipitate formation can occur also at high temperature oxidation if the dose is high enough to exceed the solid solubility. Oxide plastic deformations, due to precipitate formation, are not completely recovered even after a long high-temperature oxidation.

Finally, a model, based on the As diffusion equation, was introduced to calculate the dopant segregation at the interface. In the model the mass conservation and the As precipitation over solid solubility are taken into account. The equations introduced are able to describe both the As accumulation at the interface for low-temperature (920 °C) oxidation and the As diffusion in the bulk at high-temperature (1100 °C) oxidation. The calculated interface As concentrations are in good agreement with the experimental ones, extracted from RBS data, and they allow one to give a physical explanation to all the different surface and interface morphologies detected by AFM and TEM analyses.

ACKNOWLEDGMENTS

The authors thank M. Furnari (CNR-IMETEM) for technical support, D. Calì and C. M. Camalleri (ST Microelectronics) for performing the oxidation processes, and S. Colonna (ESRF GILDA) and S. Mobilio (Università di Roma III) for assistance with the EXAFS measurements and data analysis. This work was partially supported by CNR, Progetto Finalizzato Materiali e Dispositivi per l'Elettronica a Stato Solido (MADESS II), and Fondo Europeo di Sviluppo Regionale.

[1] A. S. Grove, O. Leistiko, Jr., and C. T. Sah, J. Appl. Phys. **35**, 2695 (1964).
[2] R. B. Fair and J. C. C. Tsai, J. Electrochem. Soc. **122**, 1689 (1975).
[3] R. B. Fair and J. C. C. Tsai, J. Electrochem. Soc. **125**, 2050 (1978).
[4] O. W. Holland, C. W. White, and S. J. Pennycook, J. Mater. Res. **3**, 898 (1988).
[5] V. Raineri, F. Iacona, F. La Via, C. M. Camalleri, and E. Rimini, in *Ion Implantation Technology 96*, edited by E. Ishida, S. Banerjee, S. Mehta, T. C. Smith, M. Current, L. Larson, and A. Tasch (IEEE, Piscataway, NJ, 1997), p. 646.
[6] F. Iacona, V. Raineri, F. La Via, and E. Rimini, J. Vac. Sci. Technol. B **16**, 619 (1998).
[7] V. Raineri, S. Lombardo, F. Iacona, and F. La Via, Nucl. Instrum. Methods Phys. Res. B **116**, 482 (1996).
[8] T. Wadsten, Acta Chem. Scand. **23**, 331 (1969).
[9] D. Nobili, S. Solmi, A. Parisini, M. Derdour, A. Armigliato, and L. Moro, Phys. Rev. B **49**, 2477 (1994).
[10] M. D. Giles, in *VLSI Technology*, edited by S. M. Sze (McGraw-Hill, New York, 1988), p. 356.
[11] L. E. Katz, in *VLSI Technology* (Ref. 10), p. 98.
[12] J. F. Götzlich, K. Habberger, H. Ryssel, H. Kranz, and E. Traumüller, Radiat. Eff. **47**, 203 (1980).
[13] E. Biermann, H. H. Berger, P. Linke, and B. Müller, J. Electrochem. Soc. **143**, 1434 (1996).
[14] P. A. Lee, P. H. Citrin, P. Eisenberger, and B. M. Kincaid, Rev. Mod. Phys. **53**, 769 (1981).
[15] *Quick Reference Manual for Silicon Integrated Circuit Technology*, edited by W. E. Beadle, J. C. C. Tsai, and R. D. Plummer (Wiley-Interscience, New York, 1985).
[16] J. L. Allain, J. R. Regnard, A. Bourret, A. Parisini, A. Armigliato, G. Tourillon, and S. Pizzini, Phys. Rev. B **46**, 9434 (1992).
[17] T. Wadsten, Acta Chem. Scand. **19**, 1232 (1965).
[18] P. C. Donohue, W. J. Siemons, and J. L. Gillson, J. Phys. Chem. Solids **29**, 807 (1968).
[19] A. Terrasi, E. Rimini, V. Raineri, F. Iacona, F. La Via, S. Colonna, and S. Mobilio, Appl. Phys. Lett. (to be published).
[20] J. C. Heyraud and J. J. Metois, Surf. Sci. **128**, 334 (1983).
[21] A. Armigliato and A. Parisini, J. Mater. Res. **6**, 1701 (1991).
[22] C. Herring, in *Structure and Properties of Solid Surfaces*, edited by R. G. Gomer and C. S. Smith (University of Chicago Press, Chicago, 1953).
[23] J. S. T. Huang and L. C. Welliver, J. Electrochem. Soc. **117**, 1577 (1970).
[24] E. C. Douglas and A. G. F. Dingwall, IEEE Trans. Electron Devices **ED-21**, 324 (1974).
[25] R. B. Fair, J. Appl. Phys. **43**, 1278 (1976).